Geophys. J. Int. (2008) **175,** 433–448 doi: 10.1111/j.1365-246X.2008.03859.x

Palaeointensity and palaeodirectional studies of early Riphaean dyke complexes in the Lake Ladoga region (Northwestern Russia)

V. V. Shcherbakova,[1] N. V. Lubnina,[2] V. P. Shcherbakov,[1] S. Mertanen,[3] G. V. Zhidkov,[1] T. I. Vasilieva[4] and V. A. Tsel'movich[1]

[1] *Geophysical Observatory 'Borok' RAS, Borok, Yaroslavskaya oblast, Russia. E-mail: grigor@borok.yar.ru*
[2] *Geological Department, Lomonosov Moscow State University, Moscow*
[3] *Geological Survey of Finland, Espoo, Finland*
[4] *Geological Institute RAS, Moscow*

Accepted 2008 May 20. Received 2008 May 20; in original form 2007 June 17

SUMMARY

Results of palaeointensity and palaeomagnetic studies for the volcanic rocks of 1450 Ma, from Early Riphaean Baltic shield dyke complex sampled in Lake Ladoga region (Karelia, Northwestern Russia) are reported. Electron microscope observations, thermomagnetic and hysteresis measurements indicate the presence of single domain (SD) to pseudo-single domain (PSD) titanomagnetite (TM) with low Ti content as the main magnetic mineral. Stepwise alternating field (AF) and/or thermal demagnetization revealed a two-component natural remanent magnetization (NRM) for most of the samples. The characteristic remanent magnetization (ChRM) component was isolated between 440 and 590 °C. Note that the ChRM amounts to 95 per cent of the NRM intensity. The geographic position of the ChRM palaeopoles does not contradict the 'key poles' of the [1270; 1580] Myr time interval, testifying anticlockwise rotation of whole East Europe Craton between 1450 and 1500 Ma. Palaeointensity determinations were performed by Coe-modified Thellier procedure. 35 samples passed our palaeointensity selection criteria and show large linear segments on Arai-Nagata plots. The site mean virtual dipole moment (VDM) varies from 2.00 to 3.91 ($\times 10^{22}$ A m^2). Based on these and other observations, we suggest that the Palaeo- and MezoProterozoic was dominated by low VDMs.

Key words: Palaeointensity; Palaeomagnetism applied to tectonics; Rock and mineral magnetism.

INTRODUCTION

The study of the ancient geomagnetic field provides valuable information about the formation and evolution of the inner solid core, the mantle and tectonic processes. There are different models describing the processes of nucleation and growth of the inner core at the early stages of the Earth's geological history and it was suggested that these processes are related to the magnitude of the geomagnetic field. The thermodynamic model of Yukutake (2000) suggests that the solid inner core started to condense from a heavy fraction of the Earth's liquid core at approximately 1200 Ma. Labrosse *et al.* (2001), determined, on the basis of their Earth cooling model, that the onset of solid core formation occurred no earlier than 2.5 Ga and suggested an age 1 ± 0.5 Ga. Hale (1987) declared, based on palaeointensity determinations, a sharp rise of geomagnetic moment at the Archean–Proterozic boundary (2500 Ma) and proposed that this event is conditioned by the onset of the solid core formation around 2550 Ma. Geodynamo modelling results also predict that the formation of the solid core is accompanied by a sharp increase in intensity of the geomagnetic dipole moment (Stevenson *et al.* 1983; Buffett *et al.* 1992; Glatzmaier & Roberts 1997). Moreover, the formation of the solid core is believed to trigger the transition of the tectonic mode from plum to plate tectonic around the Archaean–Proterozic boundary (e.g. Khain 2001). The subsequent tectonic evolution of the Earth consists mainly of the further development of plate tectonics and gradual increase of lithosphere depth (Khain 2001).

Various models predict different formation times of the Earth's solid core. Understanding the temporal evolution of geomagnetic field during the Archaean and Proterozic is essential to any solid-core formation model. However, the current paucity of palaeointensity data in the Precambrian does not allow any robust conclusions to make about the geomagnetic field at this time. For this time period, covering almost 90 per cent of the Earth's history, only about 150 palaeointensity determinations have been published (these data can be found elsewhere, for example, in the world palaeointensity databases http://wwwbrk.adm.yar.ru/palmag/index.html or ftp://ftp.ngdc.noaa.gov/seg/potfid/paleo.html). Applying only a mild selection criterion to the data drastically reduces this number (Perrin & Shcherbakov 1997). Dunlop & Yu (2004) applied their own selection criteria and found only 24 Thellier-type reliable palaeointensity determinations for the Precambrian. There are also large time intervals with no published Thellier-type palaeointensity data. In particular, there is a lack of data for the Middle and Early Proterozoic periods. Three new palaeointensity results were reported by Shcherbakova *et al*. (2004, 2006a, b) for this time interval, which fill partly the gap between 1459 and 1850 Ma.

Shcherbakova *et al*. (2004) investigated a 1770 Myr old gabbro-dolerite sill in Rybreka (South Karelia). Thellier experiments were successful for 21 out of 50 samples, and a low virtual dipole moment (VDM) of $(2.2 \pm 0.15) \times 10^{22}$ A m^2 was calculated for the high temperature (400–600 °C) natural remanent magnetization (NRM) component.

A very low average VDM of $(1.2 \pm 0.17) \times 10^{22}$ A m^2 was obtained from 14 successful samples from lava flows of the Salmi suite, South Karelia, dated at 1460 Ma (Shcherbakova *et al.* 2006a). This value may be slightly underestimated because the ferrimagnetic remanence carriers in these rocks consist of a pseudo-single domain (PSD)–multidomain (MD) magnetite mixture and the error of determination of H_{anc} for MD grains may amount to 20 per cent (Shcherbakov & Shcherbakova 2001).

An 1850 Myr old granite intrusion on the southern Siberian was studied by Shcherbakova *et al*. (2006b). A peculiarity of this collection is that NRM is characterized by quite narrow interval of blocking temperatures, T_{b}, in the vicinity of T_{c}, Curie temperature of magnetite. Because of the large size of the intrusion, the palaeointensity determined on 11 successful samples was corrected for the cooling rate which was estimated as $\sim 10^{-12}$ °C s^{-1}. After the correction, the average VDM reduced from 7.05×10^{22} A m^2 to $(5 \pm 1) \times 10^{22}$ A m^2.

The Global Palaeomagnetic database (Pisarevsky & McElhinny 2003) contains more than 250 palaeomagnetic directions for Archean–Proterozoic time. The majority of data for the East European Craton (EEC), for this time interval, are obtained from Swedish and Finish rocks. 'Key poles' for the EEC are defined for 1200–2000 Ma time interval (Buchan *et al.* 2000), but the distribution of the poles is quite irregular in time. Note that different 'key poles' were also reported by Buchan *et al.* (2000) and Pesonen *et al.* (2003) for the interval from 1270 to 1580 Ma.

The aim of this study is to improve the present palaeodirectional and palaeointensity databases for the Middle Proterozoic through detailed investigations of dated rocks from the Early Riphaean dyke complex, sampled in the Lake Ladoga region (Karelia, Northwestern Russia). The latitude and longitude of the studied area are 61°35.4′N and 30°42.0′E, respectively.

GEOLOGICAL BACKGROUND AND SAMPLING DETAILS

The EEC was formed after final amalgamation of the three segments—Fennoscandia, Volgo-Uralia and Sarmatia—occurred between 1700 and 1800 Ma (Gorbachev & Bogdanova 1993). After the collision, the development of eastern and western margins differed from the development of the interior of the EEC. The evolution of the craton is reconstructed by several well-defined stages of magmatic activity, crust deformation and sedimentation (Bogdanova *et al.* 2003, 2005). The Early Riphaean stage is characterized by compression in the northern, western and southwestern parts of the EEC, whereas rifting and passive margin occurred in its eastern part. Such events should be resolvable from rocks formed during the development of the EEC, and these also record the geomagnetic field at this time. A new palaeomagnetic study of the Lake Ladoga outcrops could yield important information about the geomagnetic field and tectonic processes during the Proterozioic.

The major tectonic mechanisms during the Post-Archean stage of Fennoscandian Shield evolution were intra- and intercratonic riftings. The Early Proterozoic endogenous events are reconstructed as a number of spatially joined or separated structures composed of volcano-terrigenous rocks (e.g. Gaál & Gorbatschev 1987; Gorbatschev & Bogdanova 1993; Nironen 1997; Lahtinen *et al.* 2005). Since the Riphaean, the magmatic activity had been characterized by the emergence of dykes, volcanic pipes and small intrusions. One of the earliest interplate magmatic units at this stage is the Rapakivi-granite-anorthosite formation, accompanied by basic and acidic dyke swarms in Southern Finland, Sweden and Western Lake Ladoga region (e.g. Åhäll & Connelly 1998; Söderlund *et al.* 2005; Brander & Söderlund 2007). The initial stage of the Riphaean rift system of the Western Fennoscandia is separated from the stage of Rapakivi-granit intrusions by the period of stabilization and erosion, during which the Rapakivi massifs were uplifted to the subsurface or surface level. The Riphaean rift system consists of series of grabens placed in Western Finland, Sweden, Western Karelia and basins at the bottom of the Bothian gulf. The terrigenous rocks of different rift system segments were dated at 1430–1450 Ma.

Magmatic complexes, synchronous with rifting, are prevalent in the Lake Ladoga region and may play a key role in our understanding of the evolutionary dynamics of the Riphaean rift system of the EEC. The Ladoga graben depression zone consists of volcano-terrigenous rocks of Early Riphaean and covering the eroded surface of the Archean and Early Proterozoic rocks, including Rapakivi granites, dated at 1546 ± 20 Ma (Salmi massif) (e.g. Svetov & Sviridenko 1995). Altered red-coloured siltstones and lava flows dated at 1499 ± 68 Ma (Bogdanov *et al.* 2003), the Valaam sills dated at 1457 ± 2 Ma, (Rämö *et al.* 2005), the Hopunvaara neck dated at 1350 Ma (Larin & Kutyavin 1993) and high-ferriferous olivine dolerites dyke complexes (sortavalites) form a narrow NNW striking belt, containing more than 10 separate bodies, confined to the NE border of the palaeorift (Fig. 1b, see e.g. Svetov 1979). Dyke bodies with two different strike directions, which probably correlate with the opening of the fault and fault zones, have been distinguished by Vasilieva & Lubnina (2006). Chemically, the dykes correspond to the Salmi basalts, whose age is therefore regarded as the age of the dykes (Vasilieva *et al.* 2001).

The first type of dykes is the western group of thin dykes, sampled on Tamkhanka (sites 1, 8) and Suur-Hapasaari (site 7) islands (Fig 1c). The dykes have a flat dip of 40°–70°. For each site, one dyke was sampled. A dyke of aphanitic dolerites on Tamkhanka Island was traced at a range of 500 m at Azimuth 335 SW, Dip 65°–70°. It has a thickness of about 1.5 m with unevenly shaped contact zones. The chilled zones are 10 to 15 cm wide and consist of glassy material with shell fractures, whereas the main part of the dykes is composed of microporphyritic plagioclase-pyroxene dolerite. At site 1, in the northern part of Tamkhanka Island, the central part of dyke, the chilled zone and the baked contact were sampled. To apply the baked contact test, samples from host rocks (gneisses of the Ladoga Formation) were sampled along a profile perpendicular to the contact line at a distance of 5–7 m. At the southern outskirts of Tamkhanka Island (site 8), samples were collected from the central part of the dyke and at distance up to 20 cm from the contact. It must be noted that rocks in the central part of this dyke were slightly changed by secondary alterations, judging from the fact that more than one palaeodirection were often isolated in the central part of the dyke whereas the margins displayed a single-component NRM.

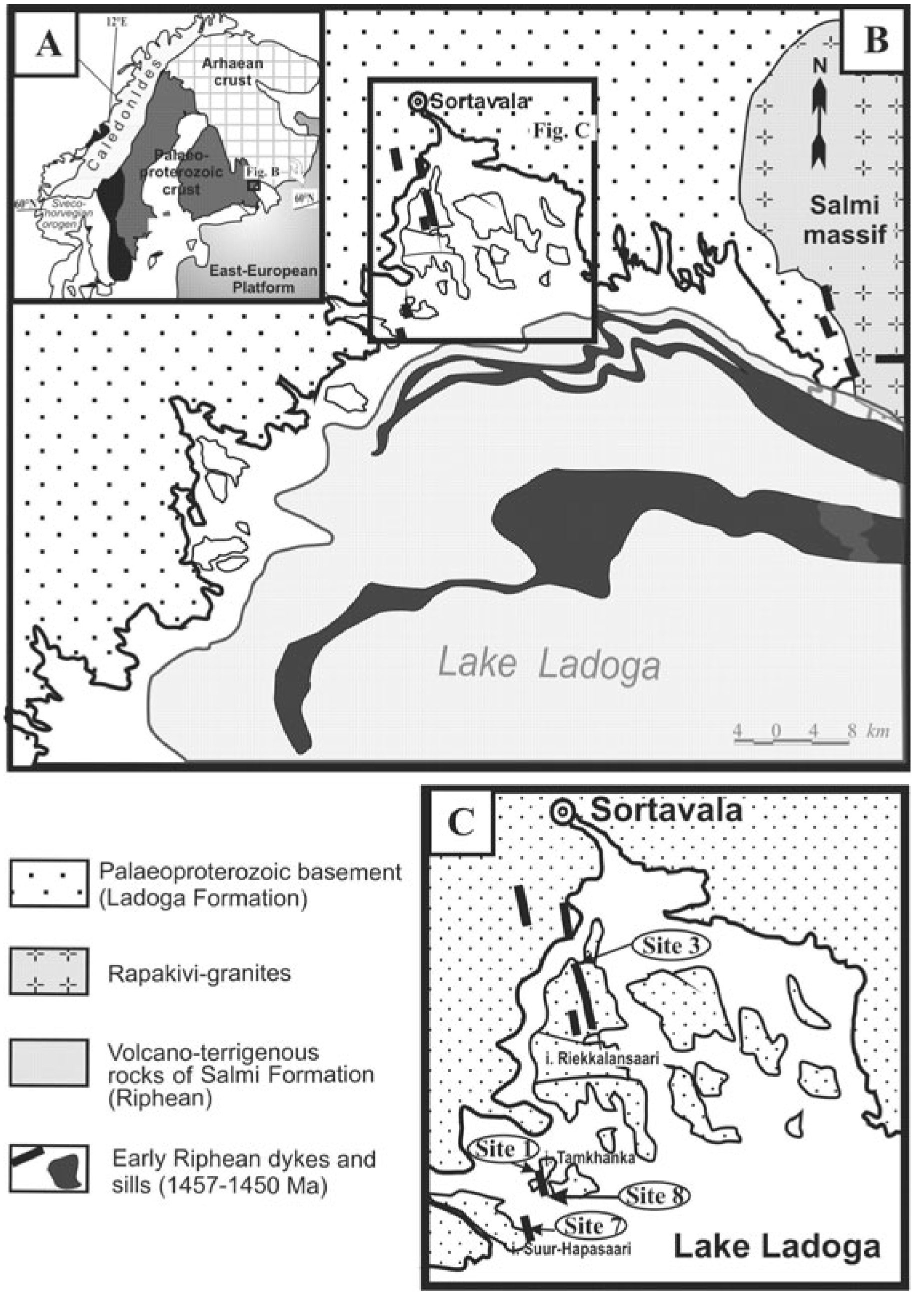

Figure 1. Location of the studied area (a), simplified geological map of the Lake Ladoga region (b) and sampling sites of the Early Riphean dyke complex (c). Site 1, Tamkhanka northern outskirts (61°35.51′N 30°41.784′E); Site 3, Riekkalansaari island (61°42.864′N 30°45.468′E); Site 7, Suur-Hapasaari island (61°34.027′N 30°42.787′E) and Site 8, Tamkhanka southern outskirts (61°35.34′N 30°41.949′E).

The dyke at Suur-Hapasaari Island (site 7) consists of a complicated dyke-vein system dipping 45°–60° in SW direction with an extension of about 50 m. Samples from the chilled zones, the central part of dyke (sample numbers from 7–15 to 7–30) and also from small apophysis of this dyke (sample numbers from 7–8 to 7–14) were collected. Samples of the host granite-gneisses of the Ladoga Formation along a profile perpendicular to the contact line at a distance up to 15 m were also taken (samples number 7-1–7-7).

The second type of dyke consists of iron rich dolerites (sortavalites) and is found on Riekkalansaari Island. Morphologically, these dykes look like plate bodies, with a thickness of up to 30 m and an extension of 30–200 m. These dykes intruded into gneisses of the Ladoga Formation and are characterised by a constant extension (strike 320°–360° and very steep 70°–80° dip towards the southwest). The dykes have chilled zones up to 15–20 cm wide, with coarse crystallised central parts. The sampling was performed mainly through the chilled zones, though some samples were taken from profiles perpendicular to the strike of dykes from the host granite-gneisses rock to determine possible secondary remagnetizations. One dyke (site 3) of this type was sampled for the palaeointensity determinations reported in this study.

Representative collections of both types of dykes from the Lake Ladoga region around the town Sortavala and from adjacent islands were collected for this study. The magnetic susceptibility, κ, was measured before the sampling directly in the outcrops using a KT-5 kappabridge. Predominantly chilled margins and backed contacts have been chosen for the sampling to define the origin of magnetization. These zones were visually identified and are also defined by a consistent decrease of κ from the contact zone to the central part of dyke. In total, more than 200 drilled cores and hand blocks oriented with a magnetic compass were collected for palaeodirectional and palaeointensity studies.

EXPERIMENTAL PROCEDURES

Palaeomagnetic experiments were carried out at the palaeomagnetic laboratory of the Geological Survey of Finland and at the All-Russia Geological Institute (Saint-Petersburg, Russia). Continuous thermomagnetic measurements and the palaeointensity experiments were performed in the Geophysical Observatory 'Borok' (Russia). Hystersis measurements were made on a Princeton Measurements corporation vibrating sample magnetometer 'Micromag' at the University of Bremen (Germany).

To assess the magnetic hardness and mineralogy of samples, measurements of magnetic susceptibility, hysteresis loop parameters such as coercive force, H_c, remanent coercive force, H_{cr}, saturation magnetization, M_s, and remanent saturation magnetization, M_{rs}, were performed. All rock magnetic and palaeomagnetic measurements were made on 4–10 cubic sister specimens of 1 cm in edge length, cut from each drilled core or hand block sample. Both reflected light and SEM of thin sections were extensively carried out to classify the geological type of the dykes and to assess possible metamorphic alterations.

The characteristic remanent magnetization (ChRM) components of the NRM were isolated by both stepwise thermal and alternating field (AF) demagnetization. The residual field in the electric oven during heatings was less than 10–15 nT. Thermochemical alteration, possibly occurring during thermal demagnetization, was monitored by measuring magnetic low-field susceptibility after each heating step, using a KLY-2 Kappa bridge. The AF cleaning was done using the 2G Enterprises three axial demagnetizer; the NRM measurements were performed on 2G Enterprises cryogenic magnetometer or on spinner magnetometer JR-5a. The results were analysed using the software package described in Enkin (1994).

The Curie points, T_c, and the thermal stability of magnetic minerals were estimated from thermomagnetic heating/cooling loops with increasing maximal temperatures, T_i. Measurements were made with a Curie balance in an external magnetic field of $H = 450$ mT. The domain structure (DS) was estimated from the Day plot (Day *et al.* 1977) and from the thermomagnetic criterion defined by Shcherbakova *et al.* (2000), which estimates the DS by thermal demagnetization of the partial thermoremanent magnetization (pTRM). The criterion relies upon the Thellier law of independence of pTRMs, respectively on the equality of blocking and unblocking temperature. The remanence remaining after the thermal demagnetization is the so-called tail of pTRM.

Shcherbakova *et al*. (2000) proposed the following procedure to measure the pTRM tail of the pTRM acquired in the temperature interval (T_1, T_2) with $T_1 > T_2$:

(1) Heating in zero field to T_c;

(2) Cooling to room temperature T_0 with the field switched on only between T_1 and T_2 [acquisition of pTRM(T_1; T_2)];

(3) Heating in zero field to T_1 [thermal demagnetization of pTRM(T_1, T_2)];

(4) Cooling in zero field to T_0 and measuring the remanence which is the tail of pTRM(T_1, T_2).

The parameter, $A(T_1,T_2) = \mathrm{tail}[\mathrm{pTRM}(T_1,T_2)]/\mathrm{pTRM}(T_1,T_2)$, measured at T_0 is used to estimate the DS. According to this definition, A is the relative value of the tail at room temperature. $A < 0.04$ means that the sample contains predominantly single domain (SD) grains, $0.04 < A < 0.15$ corresponds to PSD grains, $A > 0.15$ indicates the presence of MD grains (Shcherbakova *et al.* 2000; Shcherbakov & Shcherbakova 2001).

A two-component induction-coil thermomagnetometer, constructed at the 'Borok' Observatory, was used for measuring the tails. The device allows to induce and to demagnetize a full TRM or various pTRMs and to measure continuously the horizontal components of the remanent magnetic moment of a specimen rotating in the horizontal plane. The noise threshold of the magnetometer is 3×10^{-9} A m^2 for a cubic specimen of 1 cm edge length. The maximum available external field, whose direction is fixed in the horizontal plane, is 0.2 mT, whereas the residual field, after the coil is switched off, is less than 100 nT.

Palaeointensity was determined following the experimental protocol of Coe's modified Thellier–Thellier procedure (Coe 1967). The experiment consists of a sequence of paired heating in air to a set of increasing temperature T_i, $i = 1, \dots n$. The first heating–cooling step to T_i takes place in zero field, the second heating is also performed in non-magnetic space followed by cooling in the laboratory field, H_{lab}, equal to 20 μT. A low external field, H_{lab}, far less than the modern Earth's field, was deliberately chosen as pilot samples yielded palaeointensities between 10 and 20 μT and, as was shown by Yu *et al.* 2004, the errors are minimized when the ancient and laboratory fields are similar. Double heating was carried out in not less than 16 steps, up to 650 °C. pTRM checks and susceptibility measurements were performed after every second step.

To improve the level of confidence in our palaeointensity determinations, two to four cubic specimens of 1 cm edge length were used from each sample to obtain more objective results. Part of the specimens were heated in an electric furnace with a residual field <50 nT, whereas the remaining specimens were subjected to Coe-modified procedure in a full-vector three component vibrating sample magnetometer (3D-VSM) constructed at the Geophysical Observatory 'Borok', Russia. The 3D-VSM is supplied with a furnace; so, it can perform a completely automated Thellier procedure. The results are recorded by a master computer, which allowed us to carry out experiments on different samples using exactly the same algorithm, without extracting/placing the specimen inside the magnetometer during a Thellier experiment. The sensitivity of the 3D-VSM is 10^{-8} A m^2 and the maximum available external (vertical) field is 0.2 mT. The remanence of those specimens heated in the electric furnace was measured with a fully computer controlled astatic magnetometer with a sensitivity of 10^{-9} A m^2. The results of the palaeointensity experiments obtained for the same sample, but from different devices and methods, agree well with each other.

Wilson's method (Wilson 1961) of palaeointensity determinations was also applied to a number of sister specimens using the same full-vector 3D-VSM. This method requires a continuous record of magnetic remanence during heating to T_c. First the NRM is demagnetized in zero field and the thermal demagnetization curve NRM(T) is obtained. During subsequent cooling from T_c, a laboratory field, H_{lab}, (either 20 or 50 μT) is applied to impress a TRM, which is then subjected to thermal demagnetization by heating to T_c. Finally, both thermal demagnetization curves NRM(T) and TRM(T) are compared to find the temperature interval, (T_{w1}, T_{w2}), ($T_{w1} < T_{w2}$), where NRM(T) is similar to TRM(T). If such an interval is found, H_{anc} can be obtained from the coefficient of similarity, $K_w = \mathrm{NRM}(T)/\mathrm{TRM}(T) = H_{\mathrm{anc}}/H_{\mathrm{lab}}$, $T \in (T_{w1}, T_{w2})$. The parameter k_{w} was accepted if there was no evidence for secondary re-heating, and the similarity of NRM(T) and TRM(T) curves was considered as an argument in favour of thermoremanent nature of the NRM.

RESULTS

Rock magnetic properties

The NRM intensity of the samples varies from site to site. For instance, granite-gneiss rocks of the Ladoga Formation are characterised by weak NRM < 0.1 mA m^{-1}, $\kappa = (140–300) \times 10^{-6}$ (SI) and the Koenigsberger ratio $Q_{\mathrm{n}} = 0.1–0.59$. Values of NRM decrease from chilled zones to central ones. On the other hand, samples collected in the northern end of the island Tamkhanka (site 1) demonstrate medium NRM values 10–27 mA m^{-1}, $\kappa = (360–770) \times 10^{-6}$ (SI) and $Q_{\mathrm{n}} = 0.52–1.14$, whereas the samples taken from the southern part of Tamkhanka possess considerably stronger NRM $= (17.6–459)$ mA m^{-1}, $\kappa = (764–3071) \times 10^{-6}$ (SI) and $Q_{\mathrm{n}} = 0.58–5.28$. The strongest samples were collected on the islands Riekkalansaari (site 3) and Suur-Hapasaari (site 7). Samples from the chilled zones have typical NRM $= (0.1–3.5)$ A m^{-1} and $\kappa = (3.9–25) \times 10^{-3}$ (SI), whereas the central areas have the NRM $= (6.5–13)$ A m^{-1} and $\kappa = (20–36) \times 10^{-3}$ (SI). A significant increase of NRM and susceptibility from chilled zones to the central parts of the dykes is observed. High Koenigsberger ratios, $Q_{\mathrm{n}} = 2–34$, indicate a high palaeomagnetic stability of NRM of these samples.

Measurements of strong field thermomagnetic curves, $M_{\mathrm{s}}(T)$, revealed that the magnetic mineralogy can differ considerably from sample to sample even within the same site. Some samples from sites 1, 3 and 8 show the presence of two magnetic phases according to their thermomagnetic curves $M_{\mathrm{s}}(T)$ as shown in Fig. 2(a) for sample 3–11. The inflexion point of $M_{\mathrm{s}}(T)$ indicates the occurrence of a phase with T_{c} of about 350 °C. Evidently the sample contains at least two magnetic mineral phases presumably titanomagnetites (TM), with high and low titanium content. Some samples show a substantial paramagnetic contribution and relatively low NRM values, which is due to a small TM concentration (Figs 2a and b). When a noteable amount of magnetic mineral with low T_{c} is present, the thermodemagnetization curves NRM(T) and TRM(T) are often not similar as is seen in the comparison of TRM(T) and normalized NRM(T) (dashed line) curves in Fig. 2(b). The dissimilarity is possibly connected to the thermal instability of the low T_{c} phase, though the $M_{\mathrm{s}}(T)$ curves would not necessarily show clear evidence for substantial alteration. Another possibility is not the thermomagnetic origin of the part of NRM related to the low T_{c} phase—it might carry chemical remanence. In any case, such samples were excluded from the Thellier experiments.

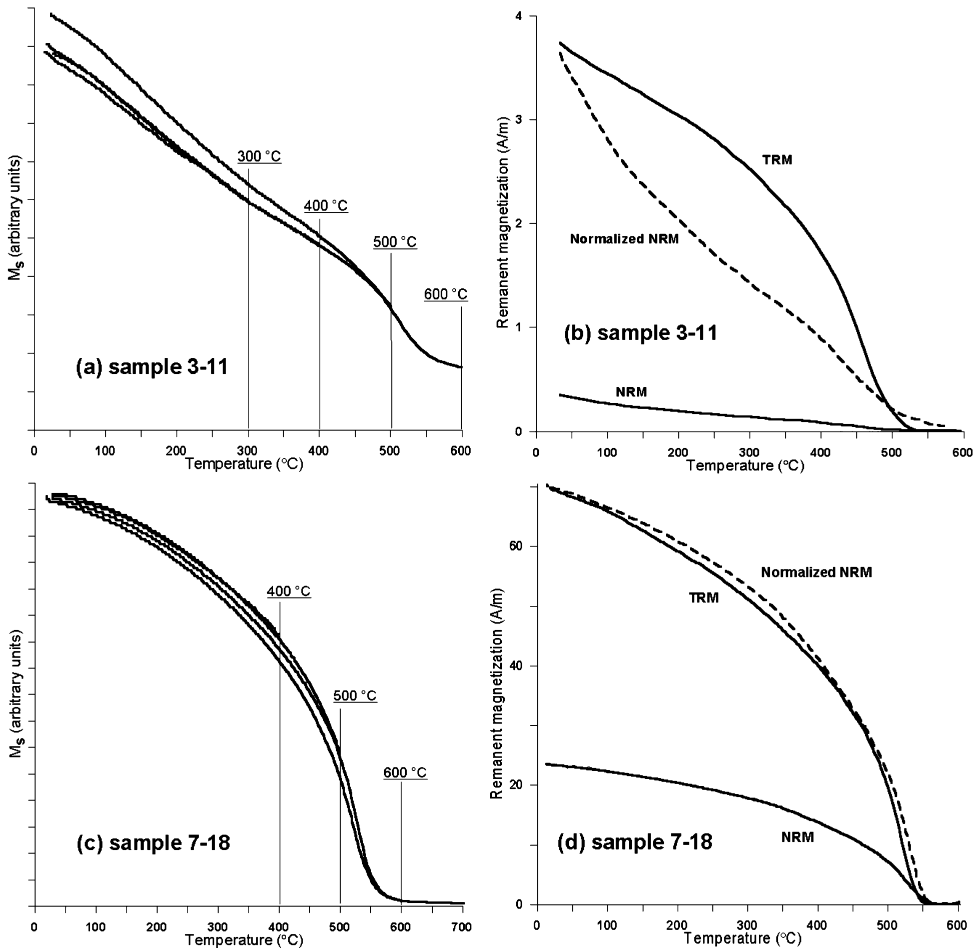

Figure 2. (a), (c) Temperature dependence of saturation magnetization in $H = 450$ mT. The set of strong field curves $M_{\mathrm{s}}(T)$ are obtained by heatings to incrementally higher temperatures, the numbers near vertical lines indicate the maximum temperatures for a given temperature loop. (b), (d) Continuous thermodemagnetization curves of NRM and TRM acquired in $H_{\mathrm{lab}} = 50$ μT (full lines). The dashed lines depict thermodemagnetization curves of NRM normalized to the corresponding TRM value measured at room temperature.

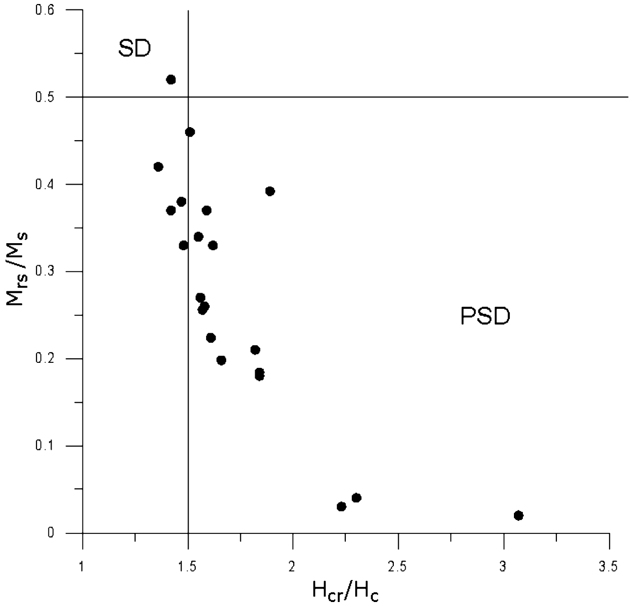

Figure 3. Day plot (Day *et al.* 1977) for samples from the sites 1, 3 and 7.

Fortunately, the majority of the samples, especially those sampled on the Suur-Hapasaari island (site 7), have a single-phase convex shape of $M_s(T)$ curves with $T_c = (540–560)$ °C, which is characteristic for low Ti titanomagnetite (e.g. Fig. 2c). Underline that the subsequent curves nicely repeat each other, proving a good thermal stability of the TM. The subsequent heating–cooling cycles show a high degree of similarity, proving the thermal stability of the TM and absence of maghaemitization. In addition, these samples typically demonstrate a good similarity between NRM(T) and TRM(T) thermomagnetic curves over a wide temperature range (Fig. 2d) pointing to a thermoremanent nature of the NRM.

To estimate the domain state, hysteresis of some of the samples from sites 1, 3 and 7 was measured. The ratios M_{rs}/M_s and H_{cr}/H_c are plotted on a Day plot (Fig. 3). As often occurs for natural samples, the ratios M_{rs}/M_s and H_{cr}/H_c fall in the SD-PSD region: $M_{rs}/M_s = 0.02–0.51$, $H_{cr}/H_c = 1.36–2.4$. Three samples with H_{cr}/H_c ratios between 2.5 and 3.1 show low MD M_{rs}/M_s.

The thermomagnetic DS test developed by Shcherbakova *et al.* (2000), confirmed the SD–PSD magnetic configuration of most of the samples. Typical examples of this test are shown in Fig. 4, for samples 3–10 and 7–29 for the pTRM(500,400) and pTRM(550,500). Both samples show hysteresis parameters typical for small PSD grains: $M_{rs}/M_s \approx 0.3$, $H_{cr}/H_c \approx 1.5$. The temperature intervals (500, 400) °C and (550, 500) °C were chosen because the blocking temperatures, T_b, of most of the samples are restricted to the interval (T_c, 400) °C. Small pTRM tails are typical of this sample set (Figs 4a, b and d). This indicates that corresponding pTRMs are carried by predominantly SD or small PSD grains. In a few cases, the tail of a relatively low temperature pTRM (400,500) was big enough to suggest the presence of PSD–MD grains in the relevant blocking temperature intervals, whereas the high temperature pTRM (550,500) demonstrated a distinctive SD-PSD behaviour of pTRM tail (Fig. 4c, sample 7–2). However, the intensity of the low temperature pTRM is always an order of magnitude less than that of the high temperature pTRM. This explains why the hysteresis parameters of these samples are usually consistent with small PSD grains. Grains of such kind can be modelled as a specific mixture of SD–PSD–MD carriers, but these carriers are physically located in the same grain.

The conclusion that two magnetic mineral phases with different Curie temperatures are present in some samples, is supported by optical and electron microscope observations of the microstructure of TM grains. In most cases, the examination of polished sections gives evidence for the existence of near-magnetite/near-ilmenite intergrowths (Fig. 5a). Electron micrographs were taken on sample 7–24 (Fig. 5b, Table 1) and energy dispersive X-ray (EDX) analysis was carried out.

As known, the oxyexsolution can continue at temperatures below the Curie point of magnetite (Dunlop & Ozdemir 1997). In this case, the ChRM would be a thermochemical remanent magnetization (TCRM) rather than TRM. However, the observation of large grain sizes near-ilmenite intergrowths and lack of fine secondary exsolution structures (Figs 5a and b) suggest a TRM origin of the NRM. Indeed, as was shown experimentally by Gapeev & Tselmovich (1983, 1986, 1992), the lower the oxidation temperature the finer the lamella, as the diffusion rate strongly increases with temperature. In particular, it was found that the appearance of exsolution lamellae with sizes more than 1 μm, like those of observed in Fig. 5(b), is a clear indication of high-temperature oxidation for primary TM formed during the initial cooling of subaerial basalts between 700 and 900 °C. In addition, the fact that Curie temperatures of all samples from our collection are lower than 600 °C, means the absence of a detectable maghemite content. This rules out the possibility of a significant chemical re-magnetization of NRM due to the process of low-temperature oxidation of near-magnetite grains. It can therefore be concluded that the primary NRM of the dykes, acquired during cooling from temperatures above T_c in the ancient field, is thermoremanent in nature and the carriers of the NRM are mainly near-magnetite SD–PSD grains originated from the high-temperature oxidation at 700–900 °C. In turn, this suggest that despite the very old age of the rocks, the stable part of the NRM (in other words, the ChRM) inherited both the palaeodirection and palaeointensity at the time of the dyke intrusion, ensuring the reliability of the results reported in this paper.

The susceptibility measurements did not show a notiable anisotropy and the same is suggested for the TRM anisotropy. Thus, an anisotropy correction was not applied on the obtained palaeointensity values.

Palaeodirectional results

The stepwise AF and/or temperature demagnetization revealed that the NRM of the most of samples mainly consists of two components. The middle-blocking temperature component (MB), is usually destroyed by heating to 400 °C or by AF demagnetization in fields less than 20 mT peak amplitude. The high-blocking-temperature component (HB) was isolated in the temperature interval 440–590 °C and/or by AF demagnetization in fields between 30 and 110 mT. The HB component is considerably more stable against both temperature and AF demagnetization, and the corresponding Zijderveld plots (Zijderveld 1967) clearly end at the origin of coordinate system when the temperature approaches T_c (Fig. 6). Component HB was identified as the ChRM. The maximum angular deviation (MAD) in all cases was less than 5°.

Dykes of the first type (Tamkhanka and Suur-Hapasaari Islands, sites 1, 7 and 8)

The NRM of these dykes is often a sum of two components. The less stable component labelled here as MB1 shows NE declination

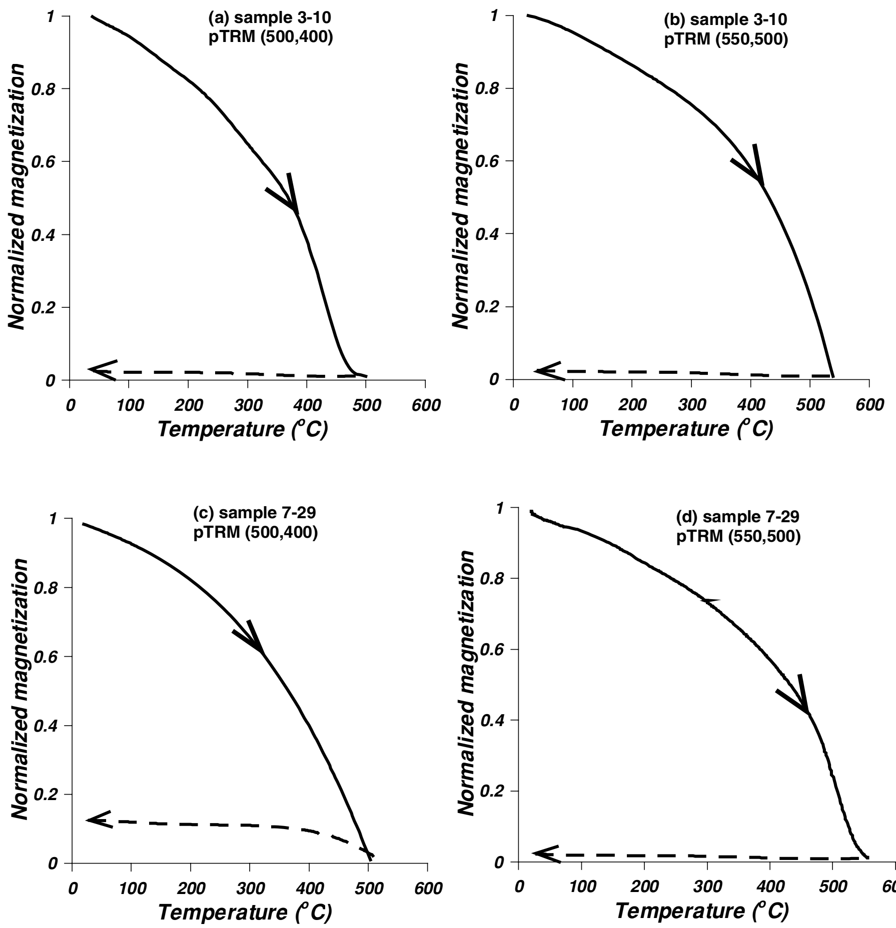

Figure 4. Application of the thermomagnetic criterion of the DS test, after Shcherbakova *et al.* (2000). Full lines are the continuous thermodemagnetization curves of the pTRMs, dashed lines are the cooling curves of the tails of the pTRMs, both heating and cooling are performed in zero field. The arrows indicate the direction of temperature change. Sample numbers and corresponding pTRMs are indicated in the Figures. $A = 0.02$ (Fig. 4a, b, d), $A = 0.13$ (Fig. 4c).

and moderate positive inclination (Figs 6a and b). On some samples, this component is not present, evidently, due to its too low intensity (Figs 6e and f). At the same time, for site 8 (Tamkhanka, southern outskirts), a part of the NRM, related to the MB1 component, increases when moving from the chilled zone to central part of the dyke. The palaeomagnetic pole recalculated from MB1-component is close to the Late Palaeozoic pole of Baltica (Smethurst *et al.* 1998).

The high-blocking temperature and coercivity component, labelled as HB1, has a NE declination and a shallow-moderate negative inclination (Figs 6a, b, e and f). The distribution of the HB1-components on a sphere is shown in Figs 7(a) and (c), the mean directions of HB1 for the sites 1, 7 and 8 are listed in Table 2.

The host granite-gneisses and gneisses of the Ladoga Formation show chemical alteration at temperatures ≈250 °C during stepwise thermodemagnetization, hence AF-demagnetization was applied to them. As for the other rocks, the majority of these samples also show two NRM components. Sample 7—1, taken from the backed granite-gneisses yield a stable consistent remanent magnetization, with a similar NE direction and shallow negative inclination (HB1-component, Figs 6c and d, Table 2). In addition to this component, samples from the baked granite-gneisses show a single polarity moderate NE direction in low AF fields and unblocking temperatures (MB1-component). Sample 7–5 taken from the unbaked gneisses of the Ladoga Formation yield two directions: in low AF fields a moderate NE direction (MB2-component, Figs 6g and h), which is close to the MB1-component in the dykes of the first type, and the second one, in high AF fields, a NW pointing low inclination direction (HB2-component, Figs 6g and h), which is clearly different from the previous direction. The result, thus, indicates that the baked contact test is positive and the NE pointing shallow remanence direction is the primary remanent magnetization of the dykes of the first type. In the unbaked gneisses samples, we additionally obtained, in low AF fields, a similar moderately NE pointing direction as MB1-direction in the dykes of the first type. Based on negative contact test, we argue for secondary origin of MB1-component of dykes.

Dykes of the second type (Riekkalansaari Island, site 3)

The samples from this site were separated into two groups, based on their NRM behaviour during thermodemagnetization and AF treatment. Samples from chilled zones form the first group with a largely single-component NRM (HB3-component) directed to the NE and slightly upwards (Figs 6i and j). Samples from the central part of the dykes of the second type form the second group and show a multicomponent NRM—a low-stability (to both AF and temperature) component of the NRM is directed towards NE, pointing downwards (MB3-component, Figs 6k and l) and high-coercivity

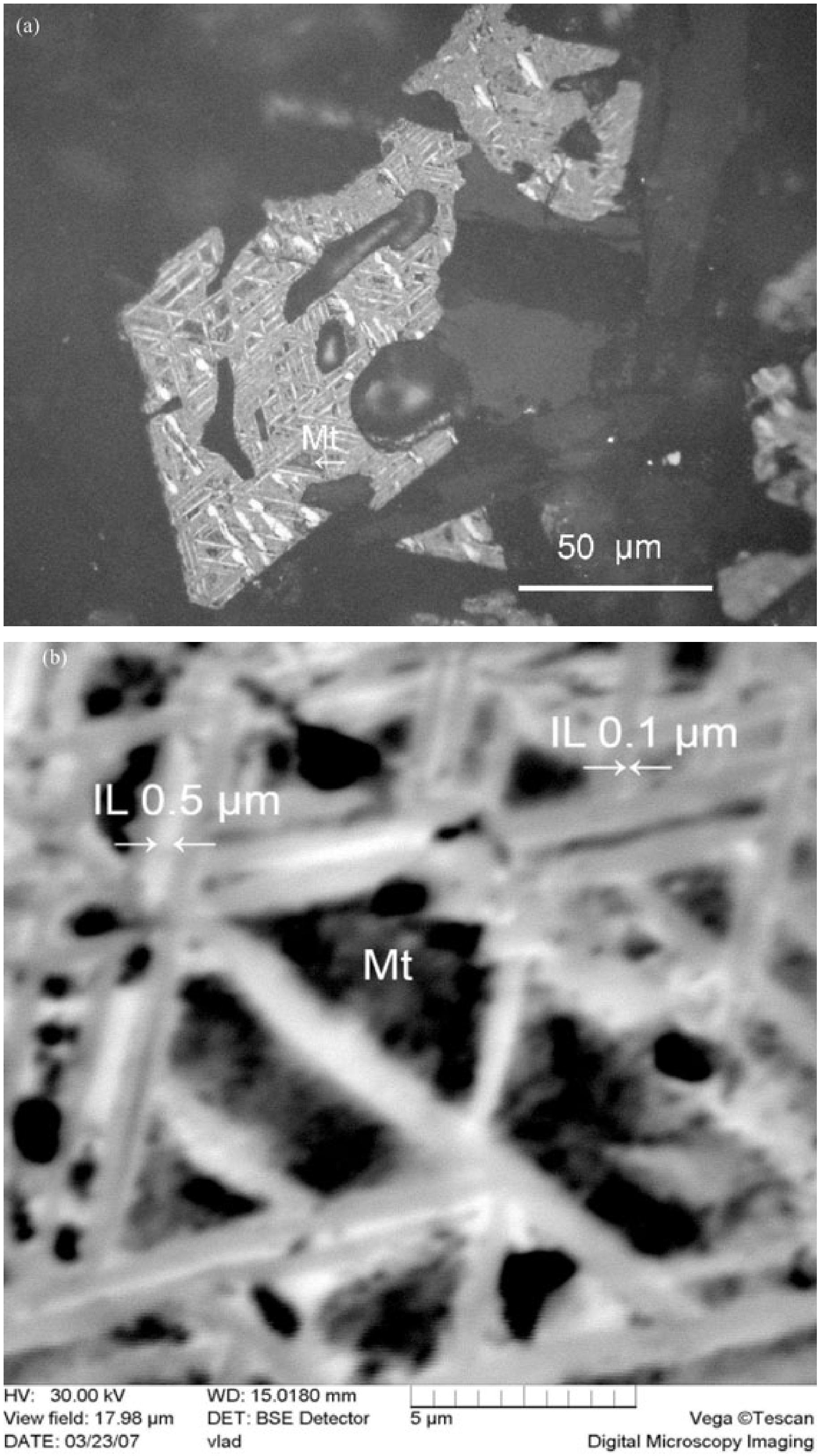

Figure 5 (a) Photomicrographs of polished section of sample 7–24. Observation of ex-solution lamellae are clear evidence for high-temperature oxidation of primary titanomagnetite. The arrow indicates a near-magnetite cell. (b) SEM backscattering image of near-magnetite cells (dark) surrounded by near-ilmenite lamellae (bright).

Table 1. Weight per cent of titanomagnetite and ilmenite in a near-magnetite cell and near-ilmenite lamella in sample 7–24. The regions analysed are indicated by arrows in Fig. 5(b).

Mineral	MgO	Al_2O_3	CaO	TiO_2	Mn	FeO	Sum
Titanomagnetite	1.21	0.96	0.24	5.37	0.50	89.11	97.39
Ilmenite	2.21	1.23	0.34	47.89	1.56	46.11	99.34

and high-temperature component with NE declination and shallow negative inclination (HB3-component, Figs 6k and l). The distribution of the HB3-component on a sphere is shown in Fig. 7(d). The mean direction of this component, listed in Table 2, is close to the direction of HB1 one (Figs 7a and d).

Unfortunately, the contact test could not be used for the dyke samples from Riekkalansaari Island to prove the primary origin of the HB3-component because the samples from the host granite-gneisses of Ladoga Formation demonstrated unstable NRM behaviour during the thermal and AF demagnetizations, both in direction and intensity. However, the similarity of the directions for both HB3 and HB1 clearly favours the primary origin of the HB3-component.

Palaeointensity results

For palaeointensity determinations and analysis, the Arai-Nagata (AN) diagrams and Zijderveld orthogonal plots (Zijderveld 1967) were constructed from the results of each experiment. The palaeointensity result for a sample was accepted only if it satisfied the following selection criteria:

(1) Thermomagnetic curves $M_s(T)$ show minor changes during the subsequent heatings (e.g. Fig. 2c). The curve must show single-phase behaviour—the sample should not show the presence of two or more magnetic minerals with different Curie points (e.g. Fig. 2a).

(2) There exists a wide enough temperature interval over which the curves NRM(T) and TRM(T) are similar (Fig. 2d).

(3) The linear fit on the AN-diagram over the temperature interval $[T_{f1},T_{f2}]$ used for the palaeointensity determination contains at least four consecutive data points.

(4) The NRM vector is univectorial over $[T_{f1},T_{f2}]$.

(5) The fraction, f, of the NRM spanned by the linear fit is not less than 20 per cent of the total NRM.

(6) The difference between the pTRM check and the pTRM acquisition, normalised to the total NRM, must be less than 5 per cent.

(7) The susceptibility remains constant, within 10 per cent, across the temperature range, (T_{f1},T_{f2}), used to determine the palaeointensity.

These criteria broadly agree with those commonly used for palaeointensity determinations (e.g. Yu & Dunlop 2001; Heunemann *et al*. 2004; Yoshihara & Hamano 2004). In addition to these criteria, we included criteria (1) and (2), which were introduced with the aim to test the thermal stability of the magnetic minerals and checking the agreement between the Wilson and the Thellier methods.

In total, 23, 21, 29 and 19 oriented hand blocks and drilled cores were taken from the sites 1, 3, 7 and 8, respectively. All these samples, without exclusion, were subjected to rock magnetic measurements and palaeointensity determinations. The application of the selection criteria resulted in six successful samples from sites both 1 and 8, eight successful samples for site 3, and 15 successful samples from site 7. The failed samples usually violated the criteria 1, 2 or 6.

Examples of accepted palaeointensity results from each site are shown in Fig. 8. The dashed line in each diagram is the linear fit to the representative points of NRM versus pTRM over the temperature interval (T_{f1},T_{f2}). As shown in Fig. 8, most of the selected specimens show a sufficiently long linear segment for reliable regression analysis. Moreover, pTRM checks plot close to the original pTRM's, which is another reliability indicator for our palaeointensity determinations and implies that thermochemical alteration was absent during the palaeointensity experiment.

The reliability of the results was also assessed by the criteria of Coe *et al*. (1978), who introduced the parameters f, g and q to characterize the quality of the results obtained. The gap factor, g, quantifies the uniformity of the distribution of successive data points in the chosen temperature interval; in the ideal case of equidistant points, $g = (N - 2)/(N - 1)$. The coefficient $k = H_{\text{anc}}/H_{\text{lab}}$ is the absolute value of the tangent of the linear fit to the AN diagram over the temperature interval (T_{f1},T_{f2}), the parameter σ is its standard error. The quality factor, $q = kfg/\sigma$, is therefore the quantitative measure of reliability of the given palaeointensity determination. As was proposed by Coe *et al.* (1978), reliable data should have the quality factor ≥ 5.

Table 3 summarises the results of 65 Thellier palaeointensity determinations for those specimens that passed the selection criteria. To avoid any misunderstanding, we stress that the data obtained from each specimen used for H_{anc} estimation was treated as an entirely independent record. To emphasize the quality of the data, we highlight the great mean fractions f of the NRM spanned by the linear fit: $f = 0.44$ for site 8, $f = 0.57$ for site 1, $f = 0.63$ for site 3 and $f = 0.7$ for site 7. It is remarkable that, in most cases, the temperature interval (T_{f1},T_{f2}) corresponds to the temperature interval of the high temperature component, HB. Almost all selected samples satisfy the criterion $q \geq 5$.

The data presented in the Table 3 are not corrected for their cooling rate, as the dykes from sites 1, 7 and 8 have a thickness of about 1 m. These dykes cooled down from T_c to about 400 °C rather rapidly, in not more than a few days, with the exception of the dyke from site 3, which has thickness ≈30 m, so, cooled over years. In these cases, a cooling rate correction is usually not applied (Dunlop & Yu 2004), though one must admit that Thellier results commonly overestimate the palaeointensity values by a few per cent. Note that the rapid cooling of the dykes provides another argument against the possibility of chemical re-magnetization process (at least in the sites 1, 7 and 8), which might take place due to the exsolution occurring below T_c. Indeed, according to detailed experiments reported by Artemova & Gapeev (1988), a (spinodal) decomposition at temperatures around 450 °C requires a much longer time—about few months.

Site averaging of H_{anc} is performed over all specimens presented in Table 3, and the results are shown in Table 4. For comparison, site averaging of H_{anc} obtained by the Wilson's method are shown in the last column of Table 4. With the exception of site 1, the results of the two methods correspond to each other rather well being statistically indistinguishable.

DISCUSSION

Palaeomagnetic directions

To constrain the age of the magnetizations, palaeomagnetic poles were calculated for the middle and high-temperature remanence components. The mean direction of the middle-blocking-temperature (MB) component corresponds to the Late Palaeozoic

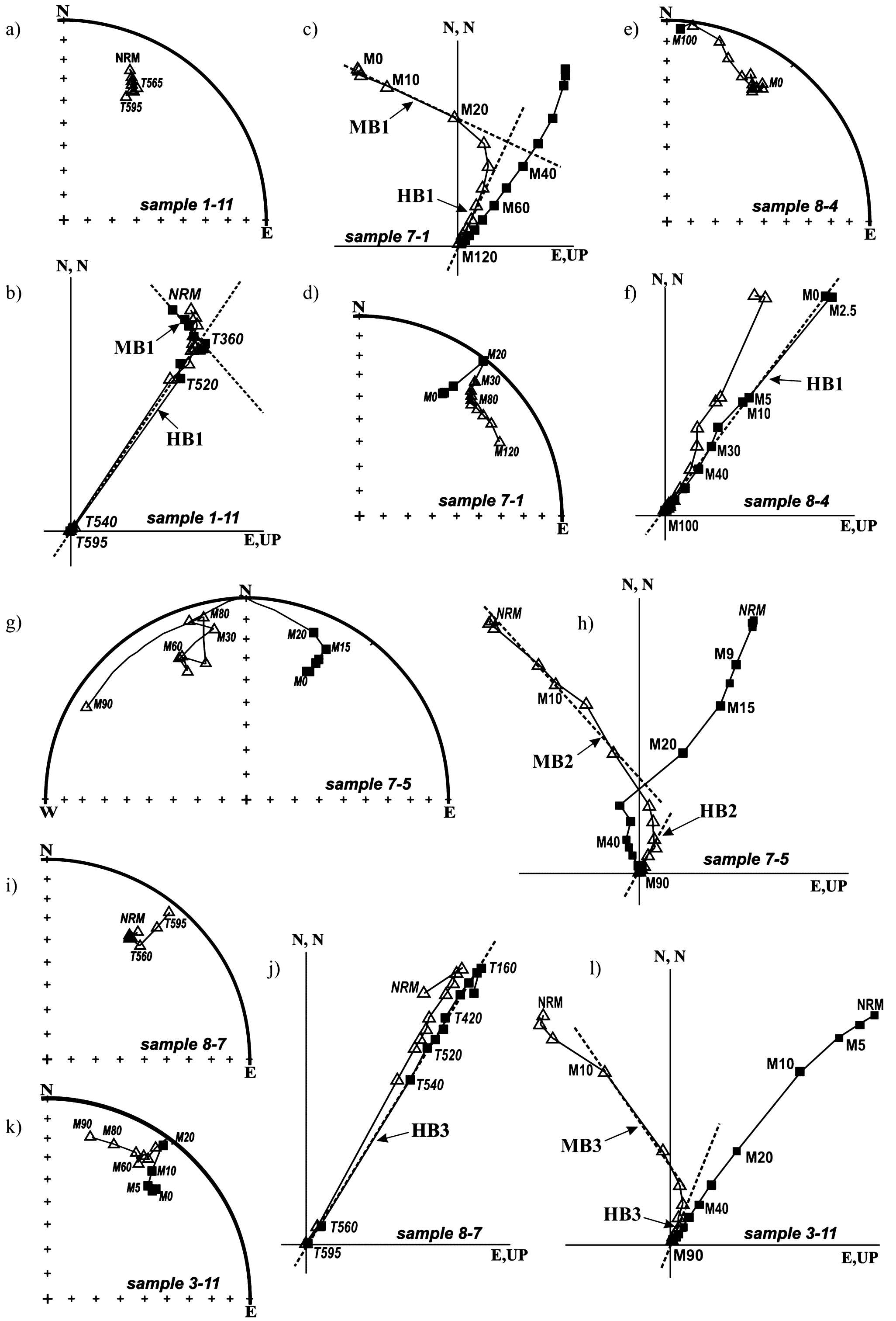

Figure 6. Examples of AF (a-h) and thermal (i-l) demagnetization behaviour of samples of the Lake Ladoga region dykes (a-b, e-f, i-l) and host granite-gneisses (c-d, g-h), plotted in: (b-c, f, h, j, l) orthogonal vector projections (Zijderveld, 1967) and (a, d-e, g, i, k) stereographic projections. Open triangle (closed squares) denote vertical (horizontal) plane. Each demagnetization step is marked by the field value (M, mT) or the temperature (T, °C). The axes on orthogonal vector projections are given in arbitrary magnetization units.

part of APWP of Baltica (Smethurst *et al.* 1998). Based on the negative backed contact test we argue that the secondary component is of the Late Palaeozoic origin.

The site-mean palaeomagnetic pole for the high-temperature component (Plat = 12.0° Plong = 175.3° $A95 = 7.5°$) is calculated for the 4 dykes of the Lake Ladoga region from the magnetization data of each sampling site (Table 2). The positive baked contact test suggests the primary origin of this component. Comparing the normal polarity pole with the Proterozoic "key" poles suggests that the new pole plots close to the group of the 1.460–1576 Ma "key"

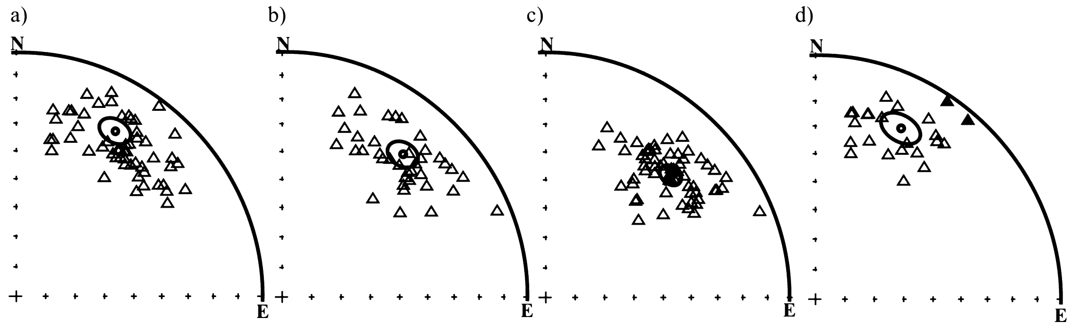

Figure 7. The distribution of high-temperature magnetization components identified *in situ*. (a) HB1-component for the Tamkhanka island, northern outskirts (dyke of first type), (b) HB1-component for the Tamkhanka Island, southern outskirts (dyke of first type), (c) HB1-component for the Suur-Hapasaari island dyke of first type and (d) HB3-component for the Riekkalansaari dyke of second type. Full (open) triangles are projections of vectors on the lower (upper) hemisphere. The small open circles represent the mean ChRM direction and the ellipses around them indicate the corresponding alpha 95 confidence region of the direction.

Table 2. The mean palaeomagnetic data for the dykes of the Lake Ladoga region (61° 35.4′N, 30° 42.0′E).

Object	SN	NC	N	Dec (°)	Inc (°)	K (°)	α_{95} (°)	Plat (N°)	Plong (E°)	dp (°)	dm (°)	$A95$ (°)
Tamkhanka northern outskirts 61° 35.51′N 30° 41.784′E	1	HB1	56	31.8	−17.1	20.5	4.3	15.4	178.0	2.3	4.4	3.2
Tamkhanka southern outskirts 61° 35.34′N 30° 41.949′E	8	HB1	40	37.2	−24.7	25.1	4.6	9.9	174.0	2.6	4.9	3.6
Suur-Hapasaari 61° 34.027′N 30° 42.787′E	7	HB1	59	45.5	−29.4	11.2	5.8	4.7	167.2	3.5	6.4	4.8
Riekkalansaari 61° 42.864′N 30° 45.468′E	3	HB3	23	29.0	−18.9	27.3	5.9	15.1	181.1	3.2	6.1	4.4
Mean of all four sites		HB	4	35.5	−22.1	90.3	9.7	11.8	175.0	5.4	10.3	7.5

SN, site's number; NC, number of the ChRM component; N, the number of samples used for palaeodirectional determinations; Dec and Inc, site-mean declination and inclination of the isolated ChRM component, respectively; K, the Fisherian concentration parameter of the individual ChRM vectors; α_{95}, the semi-angle of the cone of confidence around the mean direction in which the true direction occurs with a confidence level of 95 per cent; Plat and Plong, latitude and longitude for the palaeomagnetic pole, respectively; dp and dm, the semi-axes of the 95 per cent confidence ellipse of the pole; $A95$, the radius of the circle of 95 per cent confidence of the pole. The ChRM component used for the determination of palaeodirections is shown in third column.

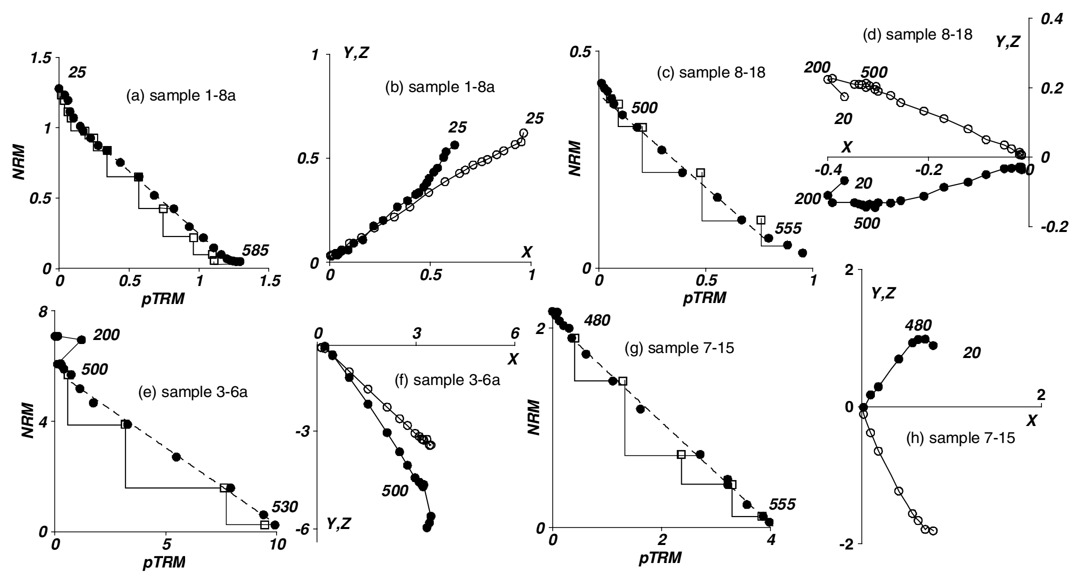

Figure 8. (a), (c), (e) and (g) are representative examples of accepted palaeointensity results. (b), (d), (f) and (h) are the corresponding orthogonal vector projection plots (in a sample's coordinate). Intensity of magnetization is given in A m^{-1}. ○ – (X,Y), ● – (X,Z).

Table 3. Results of the palaeointensity experiments.

Specimen number	T_{f1}, T_{f2} (°C)	Np	g	q	f	k	H_{anc} (μT)	σ (μT)
				Tamkhanka northern outskirts—Site 1				
1–2	520–575	11	0.87	17.1	0.62	0.72	14.4	0.02
1–4a	520–570	10	0.87	22.2	0.85	0.74	14.9	0.02
1–4b	500–555	7	0.76	18.1	0.48	0.82	16.4	0.05
1–5	535–570	8	0.85	7.3	0.32	0.53	10.6	0.02
1–8a	410–570	16	0.91	48.2	0.79	0.89	17.8	0.01
1–8b	500–560	6	0.75	26.9	0.75	0.75	14.9	0.02
1–8c	520–590	6	0.63	5.0	0.69	0.74	14.7	0.06
1–12	530–570	9	0.86	5.6	0.45	0.59	11.9	0.04
1–18a	500–590	11	0.85	23.8	0.77	0.85	17.0	0.02
1–18b	500–520	4	0.63	3.16	0.57	0.90	18.0	0.10
				Tamkhanka southern outskirts—Site 8				
8–2a	475–550	9	0.84	10.9	0.57	0.81	16.2	0.05
8–2b	505–550	10	0.88	4.3	0.60	0.64	12.9	0.08
8–2c	475–540	7	0.81	3.0	0.30	0.60	11.9	0.05
8–3	490–550	7	0.81	8.1	0.31	0.45	8.8	0.03
8–7a	500–545	7	0.82	4.4	0.29	0.71	14.2	0.04
8–7b	500–545	7	0.82	2.5	0.23	0.53	10.6	0.04
8–9a	510–535	4	0.63	4.5	0.45	0.40	8.1	0.03
8–9b	500–540	9	0.86	7.3	0.32	0.48	9.4	0.02
8–14	475–575	14	0.87	8.3	0.47	0.65	13.1	0.03
8–18	450–555	15	0.88	30.8	0.85	0.47	9.2	0.00
				Riekkalansaari—Site 3				
3–4a	490–530	8	0.84	20.2	0.66	0.32	6.4	0.01
3–4b	500–520	5	0.61	8.6	0.77	0.35	7.1	0.02
3–5	490–525	7	0.80	7.5	0.28	0.31	6.3	0.01
3–6a	490–530	8	0.84	21.6	0.77	0.56	11.1	0.02
3–6b	540–580	7	0.70	4.1	0.55	0.48	9.6	0.04
3–10a	470–520	7	0.81	8.7	0.6	0.52	10.4	0.03
3–10b	450–540	7	0.82	7.1	0.61	0.44	8.8	0.03
3–11	450–525	9	0.86	11.4	0.77	0.31	6.2	0.02
3–13a	400–525	8	0.81	26.4	0.82	0.39	7.8	0.01
3–13b	450–540	7	0.78	6.0	0.50	0.43	8.6	0.03
3–18a	400–535	12	0.85	46.8	0.85	0.44	8.9	0.01
3–18b	520–555	6	0.78	9.8	0.66	0.29	5.9	0.02
3–21	470–515	6	0.77	20.8	0.65	0.37	7.4	0.01
				Suur-Hapasaari—Site 7				
7–8	500–560	4	0.63	7.3	0.65	0.50	9.9	0.03
7–9	555–600	10	0.85	5.5	0.57	0.50	10.1	0.04
7–10a	500–600	9	0.80	14.9	0.96	0.77	15.4	0.04
7–10b	530–590	9	0.85	9.3	0.73	0.62	12.4	0.04
7–11a	520–560	4	0.61	4.7	0.44	0.52	10.4	0.03
7–11b	530–610	10	0.80	31.7	0.94	0.64	12.9	0.02
7–11c	530–610	10	0.86	11.7	0.80	0.58	12	0.03
7–12a	540–610	7	0.80	8.3	0.88	0.75	15	0.06
7–12b	530–600	10	0.69	10.8	0.85	0.77	15.3	0.06
7–12c	510–565	10	0.86	38.5	0.93	0.50	10	0.01
7–13	450–590	9	0.82	19.2	0.70	0.46	9.8	0.01
7–15a	470–520	5	0.68	11.5	0.20	0.58	11.5	0.01
7–15b	480–555	11	0.86	41.5	0.90	0.51	10.2	0.01
7–15c	300–550	10	0.83	78.1	0.98	0.71	14.3	0.01
7–17	570–610	5	0.72	4.24	0.45	0.88	17.6	0.07
7–18a	550–610	9	0.74	8.8	0.84	0.93	18.5	0.01
7–18b	540–610	9	0.78	59.4	0.84	0.83	16.6	0.01
7–20	535–570	8	0.86	9.3	0.39	0.82	16.5	0.03
7–21	510–545	11	0.86	16.8	0.87	0.71	14.2	0.03
7–23a	565–610	6	0.67	9.1	0.68	1.08	21.6	0.05
7–23b	560–610	8	0.77	10.7	0.74	1.22	24.3	0.06
7–24a	545–595	11	0.88	15.8	0.58	1.02	20.4	0.03
7–24b	575–610	5	0.66	16.8	0.60	1.19	23.7	0.03
7–24c	560–610	7	0.73	28.3	0.79	1.30	26	0.03
7–24d	575–610	5	0.66	16.8	0.59	1.19	23.7	0.03
7–25a	500–580	10	0.76	23.7	0.84	0.61	12.3	0.02

Table 3. (*Continued*.)

Specimen number	T_{f1},T_{f2} (°C)	Np	g	q	f	k	H_{anc} (μT)	σ (μT)
7–25b	565–600	5	0.61	6.2	0.71	0.82	16.4	0.06
7–25c	560–610	8	0.76	28.4	0.86	0.80	15.9	0.02
7–28a	485–585	10	0.86	29.9	0.75	0.94	18.9	0.02
7–28b	520–570	8	0.81	16.2	0.63	0.82	16.4	0.03
7–29a	530–600	10	0.77	6.9	0.67	0.74	14.7	0.05
7–29b	520–600	4	0.64	3.7	0.27	0.73	14.6	0.03
7–29c	460–585	9	0.75	103.0	0.66	0.81	16.1	0.00

Np, the number of successive data points in the interval (T_{f1},T_{f2}) used for the calculation of H_{anH}.

Table 4. Average means of H_{anc} ($\pm$ standard deviation) obtained by Thellier's and Wilson's methods and averaged virtual dipole moment (VDM).

Number of site	N_{Th}/ n_{Th}	H_{anc} (μT) (Thellier method)	VDM ($\times 10^{22}$ A m^2) (Thellier method)	N_W/ n_W	H_{anc} (μT) (Wilson's method)	VDM ($\cdot 10^{22}$ A m^2) Wilson's method)
1 – Tamkhanka northern outskirts	6/10	15.06 ± 2.40	3.76 ± 0.60	6/7	10.2 ± 0.9	2.5 ± 0.2
8 – Tamkhanka southern outskirts	6/10	11.40 ± 2.65	2.75 ± 0.64	6/6	9.4 ± 0.9	2.3 ± 0.2
3 – Riekkalansaari	8/13	8.10 ± 1.68	2.01 ± 0.42	6/6	7.5 ± 0.8	1.8 ± 0.2
7 – Suur-Hapasaari	15/32	15.90 ± 4.5	3.71 ± 1.05	19/33	14.5 ± 0.5	3.4 ± 0.1

N_{Th}, the number of samples; n_{Th}, the number of specimens used for the palaeointensity determinations by Thellier method; N_W, the number of samples; n_w, the number of specimens used for the palaeointensity determinations by Wilson's method.

poles (Buchan *et al.* 2000) and is located between the normal-polarity pole for the Valaam sill (Plat = 13.8°N Plong = 166.4°E $A95$ = 2.4°, Salminen & Pesonen 2007) and the reversed-polarity pole for the Salmi basalts (Plat = 6°N Plong = 200°E $A95$ = 11°, Shcherbakova *et al.* 2006a).

According to the new palaeomagnetic data for the dyke complex of the Lake Ladoga region, the EEC was located on between 7 deg S and 11 deg S.

Palaeointensity determinations

The VDMs calculated from the site-mean Thellier-type palaeointensities and site-mean palaeoinclinations (Table 2), are presented in Table 4. The VDM values range from 2.0×10^{22} to 3.9×10^{22} A m^2 and indicate a rather low dipole moment compared with the present day value of about 8×10^{22} A m^2. Summarizing results of this paper and the three above cited papers by Shcherbakova *et al.* (2004, 2006a, b), we obtained an average VDM of about 2.7×10^{22} A m^2 for the time interval 1450–1850 Ma, which is about half the average for the Phanerozoic value (Selkin & Tauxe 2000). Low VDM values are not a surprise for the Archean–Proterozoic; the majority of data in the Proterozoic falls in low VDM segment of the histogram shown in the inset of Fig. 9. Fig. 9 shows Archaean/Proterozoic palaeointensity data that satisfy the reliability criteria formulated by Perrin & Shcherbakov (1997). These criteria are: only thermal Thellier-type determinations are considered; at least three samples are used for the VDM calculation and the standard error of site averaging of H_{anc} should not exceed 15 per cent (the criterion of internal convergence). Thirty-four Thellier-type palaeointensity determinations passed the selection criteria. Note the data reported by Hale (1987) did not pass the criteria; so, they were not included in the compilation. The NRM of these samples is also thought to be a combination of a TRM, a CRM and a thermoviscous remagnetization (Smirnov *et al.* 2003; Dunlop & Yu 2004).

For rocks younger than 1350 Ma, a gradual increase of VDM (Fig. 9) has been observed. This could support the hypothesis that the solid inner core was formed no earlier than the Late to Middle Proterozoic (Labrosse *et al.* 2001). Contrary to the idea of low VDMs in the Archean and Early Proterozoic subsequently followed by high values in Late-/Middle- Proterozoic, high VDMs were reported for the Late Archean by Yoshihara & Hamano (2000) and Smirnov *et al.* (2003). Data, older than 3000 Myr, show low Earth dipole intensity again. However, the paucity of palaeointensity data for the Archaean and Proterozoic era makes it difficult to justify making robust conclusions about the nature of the geomagnetic field at this time.

In addition, note that despite the common palaeomagnetic praxis to calculate the VDM for the Archaean and Proterozoic, the validity of the geocentric axial dipole (GAD) hypothesis itself can be doubted for this time period. Indeed, the GAD has not been confirmed for times more than 400 Ma (McElhinny 2007) due to an insufficient number of data points. On the other hand, the analysis presented by Dunlop & Yu 2004, brought them to the conclusion 'that the Precambrian field was not markedly less dipolar than the recent field'. In other words, for the present moment there are no firm evidence either 'pro' or 'contra' the GAD hypothesis. Thus, we cannot rule out the possibility that the great dispersion of VDM values, obtained by different authors, may be an indication of non-dipolar behaviour of the overall geomagnetic field.

CONCLUSIONS

The extensive palaeomagnetic investigation of Early Riphaean dyke complexes of known age in the Lake Ladoga Region (Russia) has improved the Precambrian palaeointensity database. For main conclusions can be made:

(1) The remanence carriers consist mainly of SD and PSD titanomagnetite, with generally low but variable titanium content, and have strong thermochemical stability.

(2) The observed magnetite-ilmenite exsolution structures, identified by SEM, favour the preservation of a stable primary high temperature NRM component.

(3) Palaeodirectional studies of the Early Riphean dyke complex of Lake Ladoga region revealed the presence of two remanence components: a high coercivity well-defined component

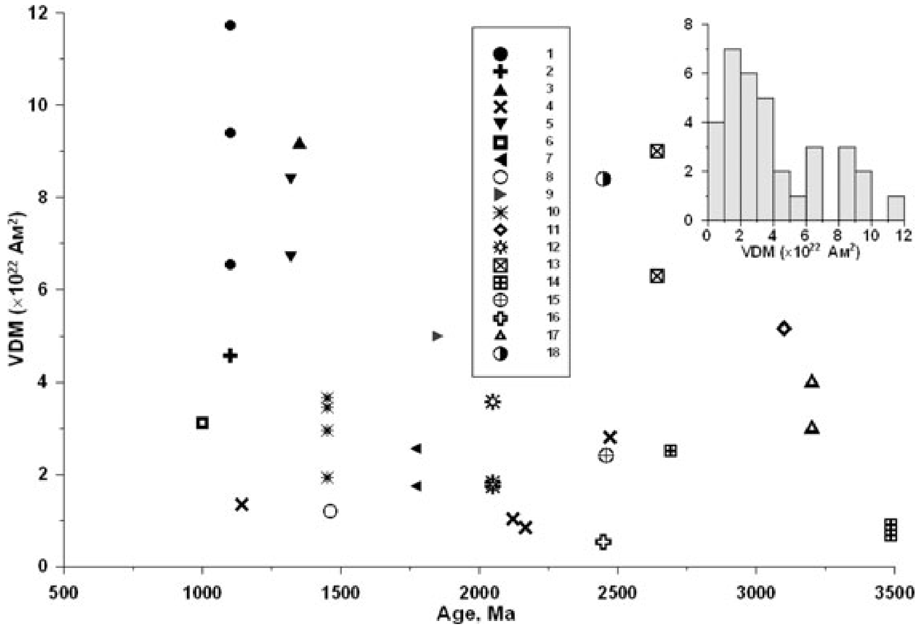

Figure 9. Selected Archaean/Proterozoic VDMs. 1, Pesonen & Halls (1983); 2, Yu & Dunlop (2001); 3, Thomas & Piper (1995); 4, Macuoin *et al.* (2003); 5, Thomas (1993); 6, Yu & Dunlop (2002); 7, Shcherbakova *et al.* (2004); 8, Shcherbakova *et al.* (2006a); 9, Shcherbakova *et al.* (2006b); 10, Shcherbakova *et al.* (this paper); 11, Bergh (1970); 12, Sumita *et al.* (2001); 13, Yoshihara & Hamano (2000); 14, Yoshihara & Hamano (2004); 15, McArdle *et al.* (2004); 16, Smirnov & Tarduno (2005); 17, Tarduno *et al.* 2007 and 18, Smirnov *et al.* 2003.

HB ($D = 35.5°$, $I = -22.1°$, $\alpha95 = 9.7°$) and a low coercivity component MB related to the Late Palaeozoic pole of Baltica (Smethurst *et al.* 1998). Positive contact test supported the primary origin of the HB-component.

(4) The HB-component yields a new palaeopole (Plat = 11.8°N, Plong = 175.0°E, $\alpha95 = 7.5°$) for East European Craton. The pole takes EEC on 9°S–13°S latitude.

(5) The obtained palaeointensity results are of reliable quality, indicate low geomagnetic field intensity. The corresponding low VDM values (2.0 to 3.8 × 10^{22} A m^2) agree with observations from previous studies of the Late and Middle Proterozoic.

ACKNOWLEDGMENTS

Thoughtful and cconstructive reviews by Simo Spassov and Maxwell Brown largely improved the paper. This work was supported by INTAS Grant 03-51-5807 and Russian Fund of Fundamental Researches Grants 03-05-64423 and 07-05-01140a. This research was supported by the Natural Sciences and Engineering Research Council of Canada through the grant A7709 to D.J.D.

REFERENCE

Artemova, T.G. & Gapeev, A.K., 1988. Decomposition of solid solutions in a magnetite-ulvospinel system, *Izvestia, Earth Phys.,* **24**(12), 1005–1010.

Aäll, K.I. & Connelly, J., 1998. Intermittent 1.53–1.13 Ga magmatism in western Baltica; age constraints and correlations within a postulated supercontinent, *Precambrian Res.,* **92,** 1–20.

Bergh, H.W., 1970. Paleomagnetism of the stillwater complex, Montana, in *Paleogeophysics,* Vol. 17, pp. 143–158, ed. Runcorn, S.K., Academic Press, London.

Bogdanov, Yu.B., Savatenkov, V.V., Ivannikov, V.V. & Frank-Kamenetsky, D.A., 2003. Isotopic age of volcanic rocks of Salmi Riphaean suite, in *Isotopic Chronology in Solution of Geodynamic and Ore Genesis,* pp. 071–072., Nauka, St-Petersburg.

Bogdanova, S.V., Kheraskova, T.N., Postnikov, A.V. & Volozh, Yu.A., 2003. Meso-Neoproterozoic Baltica: interior part and margins, Magmatism on passive margin of Rodinia (IGSP project 440), pp. 006–007, GI UNC RAN, Ufa.

Bogdanova, S.V., Gorbatschev, R. & Garetsky, R.G., 2005. The East European Craton, in *Encyclopedia of Geology,* Vol. 2, pp. 034–049, eds Selley, R.C., Cocks, L.R., Plimer, I.R., Elsevier, Amsterdam.

Brander, L. & Söderlund, U., 2007. Mesoproterozoic (1.47–1.44 Ga) orogenic magmatism in Fennoscandia; baddeleyite U-Pb dating of a suite of massif-type anorthosite in S Sweden, *Int. J. Earth Sci.*, doi: 10.1007/s00531-007-0281-0, Springer, Berlin.

Buchan, K.L., Mertanen, S., Park, R.G., Pesonen, L.J., Elming, S.-A., Abrahamsen, N. & Bylund, G., 2000. Comparising the drift of Laurentia and Baltica in the Proterozoic: the importance of key palaeomagnetic poles, *Tectonophysics,* **319**(3), 167–198.

Buffett, B.A., Huppert, H.E., Lister, J.R. & Woods, A.W., 1992. Analytical model for solidification of the Earth's core, *Nature,* **356**(6367), 329–331.

Coe, R.S., 1967. The determination of paleointensities of the Earth magnetic field with special emphasize on mechanisms which could cause nonideal behavior in Thelliers method, *J. Geomag. Geoelectr.,* **019,** 157–179.

Coe, R.S., Gromme, C.S. & Mankinen, E.A., 1978. Geomagnetic paleointensities from radiocarbon-dated lava flows on Hawaii and the question of the Pacific nondipole low, *J. geophys. Res.,* **083,** 1740–1756.

Day, R.S., Fuller, M. & Schmidt, V.A., 1977. Hysteresis properties of titanomagnetites: grain size and composition dependence, *Phys. Earth planet. Inter.,* **013,** 260–267.

Dunlop, D. & Ozdemir, O., 1997. *Rock Magnetism. Fundamentals and Fronteirs,* Cambridge University Press, Cambridge.

Dunlop, D. J. & Yu, Y., 2004. Intensity and polarity of the geomagnetic field during precambrian time, in *Timescales of the Internal Geomagnetic*

Field, Geophys. Monograph. Series, Vol. 145, pp. 85–100, ed. Channel, J.E.T., Kent, D.V., Lowrie, W. & Meert, J.G., AGU, Washington, DC.

Enkin, R.J., 1994. *A Computer Program Package for Analysis and Presentation of Paleomagnetic Data,*Pacific Geoscience Centre, Geol. Surv. Can.

Gaál, G. & Gorbatschev, R., 1987. An outline of the Precambrian evolution of the Baltic Shield, *Precambrian Res.,* **35,** 15–52.

Gapeev, A.K. & Tselmovich, V.A., 1983. Microtexture of synthetic titanomagnetite oxidized at high partial pressures of oxygen, *Izvestia, Earth Phy,,* **19**(22), 983–986.

Gapeev, A.K. & Tselmovich, V.A., 1986. Microstructure of natural heterophasically oxidized titanomagnetites, *Izvestia, Earth Phys.,* **22**(4), 331–334.

Gapeev, A.K. & Tselmovich, V.A., 1992. The microstructure and domain structure of multiphase oxidized titanomagnetites, *Phys. Earth planet. Inter.,* **70,** 243–247.

Glatzmaier, G.A. & Roberts, P.H., 1997. Simulating the Geodynamo, *Contemp. Phys.,* **38,** 269–288.

Gorbachev, R. & Bogdanova, S., 1993. Frontiers in the Baltic Shield, *Precambrian Res.,* **64,** 3–21.

Hale C.J., 1987. Paleomagnetic data suggest link between the Archean-Proterozoic boundary and inner-core nucleation, *Nature,* **329,** 233–237.

Heunemann, C., Krasa, D., Gurevitch, E.L., Soffel, H.C. & Bachtadse, V., 2004. Directions and intensities of the Earth's magnetic field during a reversal: results form the Permo-Triassic Siberian Trap Basalts, Russia, *Earth planet. Sci. Lett.,* **218,** 197–213.

Khain, V.E., 2001. *Tectonics of Continents and Oceans (2000),* Scientific World, Moscow.

Labrosse, S., Poirier, J.-P. & Le Mouel, J.-L., 2001. The age of the inner core, *Earth planet. Sci. Let.,* **190**(3–4), 111–123.

Lahtinen, R., Korja, A. & Nironen, M., 2005. Paleoproterozoic tectonic evolution, in *Precambrian Geology of Finland—Key to the Evolution of the Fennoscandian Shield,* pp. 481–532, eds Lehtinen, M., Nurmi, P.A., Rämö, O.T. Elsevier, Amsterdam.

Larin, A.M. & Kutyavin, E.P., 1993. The age of Jotnian magmatism of Lake Ladoga region, *Stratigr. Geol. Corr.,* **1**(5), 336–347.

Macuoin, M., Valet, J.P., Besse, J., Buchan, K., Ernst, R., Le Goff, M. & Scharer, U., 2003. Low Paleointensities recorded in 1 to 2.4 Ga Proterozoic dykes, Superior Province, Canada, *Earth planet. Sci. Lett.,* **213,** 79–95.

McArdle, N. J., Halls, H.C. & Shaw, J., 2004. Rock magnetic studies and a comparison between microwave and Thellier palaeointensities for Canadian Precambrian dykes, *Phys. Earth planet. Inter.,* **147,** 247–254.

McElhinny, M.W., 2007. Geocentric axial dipole hypothesis, in *Encyclopedia of Geomagnetism and Paleomagnetism,* pp. 281–286, eds Gubbins, D. & Herrero-Bervera, E., Springer, Dordrecht.

Nironen, M., 1997. The Svecofennian Orogen: a tectonic model, *Precambrian Res.,* **86,** 21–44.

Perrin, M. & Shcherbakov, V.P., 1997. Palaeointensity of the earth's magnetic field for the Past 400 Ma: evidence for a dipole structure during the Mezozoic low, *J. Geomag. Geoelectr.,* **049,** 601–614.

Pesonen, L.J. & Halls, H.C., 1983. Geomagnetic field intensity and reversal asymmetry in late Precambrian Keweenawan rocks, *Geoph. J. R. astr. Soc.,* **73,** 241–270.

Pesonen, L.J. *et al.*, 2003. Palaeomagnetic configuration of continents during the Proterozoic, *Tectonophysics,* **375**(1–4), 289–324.

Pisarevsky, S. & McElhinny, M.W., 2003. Global paleomagnetic visual database, *EOS, Trans. Am. geophys. Un.,* **84**(20), 192.

Rämö, O.T., *et al.*, 2005. Mesoproterozoic CFB magmatism in the Lake Ladoga basin, Russian Karelia, in *Proceedings of the Fifth Dyke Conference 31.7–3.8. 2005,* Rovaniemi, Finland, 41 pp.

Salminen, J. & Pesonen, L.J. 2007. Paleomagnetic and rock magnetic study of the Mesoproterozoic sill, Valaam island, Russian Karelia, *Precambrian Res.,* **159,** 212–230.

Selkin, P.A. & Tauxe, L., 2000. Long-Term variations in palaeointensity, *Phil. Trans. R. Soc. Lond., A.,* **358,** 1065–1088.

Shcherbakov, V.P. & Shcherbakova, V.V., 2001. On suitability of the Thellier method of paleointensity determinations to pseudosingledomain and multidomain grains, *Geophys. J. Int.,* **146,** 20–30.

Shcherbakova, V.V., Shcherbakov, V.P. & Heider, F., 2000. Properties of partial thermoremanent magnetization in PSD and MD magnetite grains, *J. geophys. Res.,* **105**(NB1), 767–782.

Shcherbakova, V.V., Zhidkov, G.V., Pavlov, V.E. & Zemtsov, V.A., 2004. Determinations of palaeointensity on Proterozoic rocks of South Karelia, in *Paleomagnetism and Rock Magnetism,* pp. 92–95, Kazan University Press, Kazan.

Shcherbakova, V.V., Pavlov, V.E., Shcherbakov, V.P., Neronov, I. & Zemtsov, V.A., 2006a. Preliminary results of paleomagnetic investigations of the Salmi suite (North Ladoga) and estimation of palaeointensity on the Early-Middle Riphaean boundary, *Izvestiya, Phys. Solid Earth, (in Russian),* **42,** 233–243.

Shcherbakova, V.V., Shcherbakov, V.P., Didenko, A.N. & Vinogradov, Y.K., 2006b. Determination of the palaeointensity in the early proterozoic from granitoids of the shumikhinskii complex of the siberian craton, *Izvestiya, Phys. Solid Earth, (in Russian),* **42,** 521–529.

Smethurst, M.A., Khramov, A.N. & Pisarevsky, S., 1998. Palaeomagnetism of the lower ordovician orthoceras limestone, St. Petersburg, and a revised drift history for Baltica in the early Palaeozoic, *Geophys. J. Int.,* **133,** 44–56.

Smirnov, A.V. & Tarduno, J. A., 2005. Thermochemical remanent magnetization in Precambrian rocks: are we sure the geomagnetic field was weak? *J. geophys. Res.,* **110,** B06103, doi:10.1029/2004JB003445.

Smirnov, A. V., Tarduno, J. A. & Pisakin, B. N., 2003. Paleointensity of the Early Geodynamo (2.45 Ga) as recorded in Karelia: a single crystal approach. *Geology,* **31,** 415–418.

Söderlund, U., Isachsen, C.E., Bylund, G., Heaman, L.M., Patchett, P.J., Vervoort, J.D. & Andersson, U.B., 2005. U-Pb baddelyite ages and Hf, Nd isotope chemistry constraining repeated mafic magmatism in the Fennoscandian Shield from 1.6 to 0.9 Ga. Contrib. *Mineral. Petrol.,* **150,** 174–194.

Stevenson, D., Spohn, T. & Schubert, G., 1983. Magnetism and thermal evolution of the terrestrial planets, *Icarus,* **054,** 466–489.

Sumita, I., Hatakeyama, T., Yoshihara, A. & Hamano, Y., 2001. Paleomagnetism of late Archean rocks of Hamersley basin, Western Australia and the paleointensity at early Proterozoic, *Phys. Earth planet. Inter.,* **128,** 223–241.

Svetov, A.P., 1979. *Platform Basalt Volcanism of the Karelides of the Karilia* (in Russian), Nauka, Leningrad.

Svetov, A.P. & Sviridenko, L.P., 1995. *Riphaean Volcano-plutonism of the Fennoscandian Shield* (in Russian), Karelian Research Centre of RAS, Institute of Geology, Petrozavodsk.

Tarduno, J.A., Cottrell, R.D., Watkeys, M.K. & Bauch, D., 2007. Geomagnetic field strength 3.2 billion years ago recorded by single silicate crystals, *Nature,* **446,** 657–660, doi:10.1038/nature05667.

Thomas, D.N., 1993. An integrated rock magnetic approach to the selection or rejection of ancient basalt samples for palaeointensity experiments, *Phys. Earth. planet. Inter.,* **075,** 329–342.

Thomas, D.N. & Piper, J.D.A., 1995. Evidence for the existence of a transitional geomagnetic field recorder in a Proterozoic lava succession, *Geophys. J. Int.,* **122,** 166–182.

Vasilieva, T.I. & Lubnina, N.V., 2006. Riphaean dyke complex of Lake Ladoga region as indicator of the beginning stage of riftogenous, in *Proceedings of XXXIX Tectonic Conference: Areas of Active Tectogenesisin Modern and Ancient History of the Earth,* Vol. 1, pp. 73–76, GEOS, Moscow.

Vasilieva, T.I., Frank-Kamenetsky, D.A. & Zayanchek, A.V., 2001. Dyke complexes as indicators of Late Proterozoic rifting (an example of Sortaval area, NW Ladoga), in *Proceedings of the 7th Zonenshain International Conference on Plate Tectonics,* pp. 222–224, Scientific World, Moscow.

Wilson, R.L., 1961. Paleomagnetism in Northern Ireland, part I: the thermal demagnetisation of natural magnetic moments in rocks, *Geophys. J. R. astr. Soc.,* 45–58.

Yoshihara, A. & Hamano, Y., 2000. Intensity of the Earth's magnetic field in late Archean obtained from diabase dikes of the Slave Province, Canada, *Phys. Earth planet. Inter.,* **117,** 295–307.

Yoshihara, A. & Hamano, Y., 2004. Palaeointensities determined from the middle Cretaceous basalt in Liaoning Province, northeastern China, *Phys. Earth planet. Inter.,* **142,** 49–59.

Yu, Y. & Dunlop, D.J., 2001. Paleointensity determination on the late Precambrian Tudor gabbro, Ontario, *J. geophys. Res.,* **106**(B11), 26 331–26 348.

Yu, Y. & Dunlop, D.J., 2002. Multivectorial palaeointensity determination from the Cordova gabbro, southern Ontario, *Earth planet. Sci. Lett.,* **203,** 983–998.

Yu, Y., Tauxe, L. & Genevey, A., 2004. Toward an optimal geomagnetic field intensity determination Technique, *Geochem. Geophys. Geosyst.* **5**(2), Q02H07, doi: 10.1029/2003GC000630.

Yukutake, T., 2000. The inner core and the surface heat flow as clues to estimating the initial temperature of the Earth's core, *Phys. Earth planet. Inter.,* **121,** 103–137.

Zijderveld, J.D.A., 1967. Demagnetisation of rocks: analysis of results, in *Methods in Paleomagnetism.,* pp. 254–286, eds Collinson, D.V., Kreer, K.M. & Runcorn, S.K., Elsevier, New York.